

The CRAC channel consists of a tetramer formed by Stim-induced dimerization of Orai dimers

Aubin Penna¹, Angelo Demuro², Andriy V. Yeromin¹, Shenyuan L. Zhang¹, Olga Safrina¹, Ian Parker^{1,2}
& Michael D. Cahalan^{1,3}

Ca^{2+} -release-activated Ca^{2+} (CRAC) channels underlie sustained Ca^{2+} signalling in lymphocytes and numerous other cells after Ca^{2+} liberation from the endoplasmic reticulum (ER). RNA interference screening approaches identified two proteins, Stim^{1,2} and Orai^{3–5}, that together form the molecular basis for CRAC channel activity^{6,7}. Stim senses depletion of the ER Ca^{2+} store and physically relays this information by translocating from the ER to junctions adjacent to the plasma membrane^{1,8,9}, and Orai embodies the pore of the plasma membrane calcium channel^{10–12}. A close interaction between Stim and Orai, identified by co-immunoprecipitation¹² and by Förster resonance energy transfer¹³, is involved in the opening of the Ca^{2+} channel formed by Orai subunits. Most ion channels are multimers of pore-forming subunits surrounding a central channel, which are preassembled in the ER and transported in their final stoichiometry to the plasma membrane. Here we show, by biochemical analysis after cross-linking in cell lysates and intact cells and by using non-denaturing gel electrophoresis without cross-linking, that Orai is predominantly a dimer in the plasma membrane under resting conditions. Moreover, single-molecule imaging of green fluorescent protein (GFP)-tagged Orai expressed in *Xenopus* oocytes showed predominantly two-step photobleaching, again consistent with a dimeric basal state. In contrast, co-expression of GFP-tagged Orai with the carboxy terminus of Stim as a cytosolic protein to activate the Orai channel without inducing Ca^{2+} store depletion or clustering of Orai into punctae yielded mostly four-step photobleaching, consistent with a tetrameric stoichiometry of the active Orai channel. Interaction with the C terminus of Stim thus induces Orai dimers to dimerize, forming tetramers that constitute the Ca^{2+} -selective pore. This represents a new mechanism in which assembly and activation of the functional ion channel are mediated by the same triggering molecule.

As an atypical four transmembrane-spanning protein with no sequence similarity to any other ion channel, the subunit organization of Orai and the mode of activation remain undefined. Knowledge of Orai stoichiometry is crucial to understanding the mechanisms of channel assembly, gating and ion permeation, but previous studies have led to differing conclusions, with biochemical experiments suggesting that the Orai complex is a dimer in both resting and thapsigargin-treated cells¹⁴, whereas functional measurements of expressed tandem Orai multimers indicate a tetramer as the active CRAC channel pore¹⁵. To resolve this issue, we began by applying biochemical techniques used in the past to solve the pore stoichiometry of other channels^{16–19}, including: co-immunoprecipitation, chemical cross-linking of intact and lysed cells, and polyacrylamide gel electrophoresis (PAGE) under non-dissociating conditions. Reciprocal co-immunoprecipitation confirmed that Orai subunits bearing different tags can co-assemble^{11,14} (Supplementary Fig. 1). After treatment of

total cell lysates from *Drosophila* S2 cells transfected with haemagglutinin (HA)-tagged Orai, increasing concentrations of three different lysine-reactive homobifunctional reagents produced cross-linked species on SDS-PAGE gels of ~80, ~120 and ~160 kDa, consistent with molecular masses of Orai dimers, trimers and tetramers, respectively (Fig. 1a). The bands corresponding to Orai dimers were invariably the most intense. This pattern was also seen in intact Orai-transfected S2 cells using both cysteine- and lysine-reactive homobifunctional cross-linkers, again suggesting that Orai dimers are the main form of the protein present in living cells (Supplementary Fig. 2a). The relative mobility of each band decreased as a logarithmic function of the estimated number of cross-linked subunits, indicating that the cross-linked products are integral homomultimers of the monomeric subunit¹⁸ (Supplementary Fig. 2b). This was confirmed using a functional GFP-Flag-tagged Orai construct (GFP-Orai); the GFP tag increased the apparent molecular mass of the Orai monomer by the predicted amount of ~26 kDa (Supplementary Fig. 2c, d). If each oligomeric species was composed purely of Orai, their sizes would be directly proportional to an integer multiple of the ~68 kDa GFP-Orai monomer, which is exactly what we observed. The absence of graded formation of oligomers with a higher order than dimers as a function of increasing cross-linker concentration (Fig. 1a and Supplementary Fig. 2a) or time of cross-linker incubation (Supplementary Fig. 3) suggests that the Orai oligomeric state is a dimer in resting S2 cells. The predominant homodimeric stoichiometry was further confirmed in S2 and human embryonic kidney HEK293 cells by perfluorooctanoic acid (PFO) native gel electrophoresis. PFO is a mild non-denaturing and non-dissociating detergent for molecular complexes that has been successfully used to determine the quaternary structure of various membrane proteins¹⁹. Under mild solubilization conditions, Orai was almost exclusively observed in a dimeric state (Fig. 1b). Varying the PFO to protein and/or lipid ratio, the time or the temperature of solubilization in PFO did not lead to the appearance of higher-order Orai oligomers (Supplementary Fig. 4).

When Stim and Orai are co-expressed in *Drosophila* S2 cells, a greatly amplified CRAC current is recorded after store depletion⁴. To analyse Orai stoichiometry when the CRAC channel is functional, we used S2 cells transfected with Stim and Orai and performed chemical cross-linking experiments on total cell lysates of resting cells and cells that had been treated with thapsigargin to deplete the Ca^{2+} stores (Fig. 1c). When Orai was transfected alone, no obvious change in the cross-linking pattern was observed with or without thapsigargin treatment. In contrast, store depletion caused a decrease in the cross-linked dimer intensity of a V5-His-tagged Stim protein expressed alone, and a decrease in the intensity of both Orai and Stim dimers in co-transfected cells. Because a constant amount of protein was loaded into each lane, most of the Stim protein, and the Orai protein when co-expressed with Stim, were probably present as

¹Department of Physiology and Biophysics, ²Department of Neurobiology and Behavior, and ³Center for Immunology, University of California Irvine, California 92697-4561, USA.

very high molecular mass cross-linked aggregates that did not enter the gel.

Because aggregation of Stim and Orai into macromolecular complexes precluded the determination of Orai stoichiometry in the active state, we sought a way to activate the CRAC channel without inducing higher order Orai cluster formation and, in addition, to test whether aggregation of Orai into punctae is a requirement for CRAC channel function. The C-terminal portion of STIM1, expressed as a cytosolic protein, activates CRAC current constitutively in Jurkat T cells²⁰ and in HEK cells co-transfected with Orai1 (refs 13 and 21). Expression of *Drosophila* C-terminal Stim bearing a V5-His tag (C-Stim) induced constitutive Ca²⁺ influx in S2 cells (Supplementary Fig. 5). We compared currents in S2 cells co-transfected with GFP-Orai and with either full-length Stim or C-Stim. When co-transfected with Stim, GFP-Orai produced an amplified CRAC current that developed on passive store depletion (Fig. 2a), which is similar in time course (half-time of 83 ± 24 s, *n* = 11 cells) but approximately tenfold larger in amplitude than native CRAC currents²² and is consistent with results described previously for Stim plus untagged Orai⁴. In contrast, cells transfected with C-Stim plus GFP-Orai showed a robust pre-activated CRAC-like current immediately on breaking-in to initiate whole-cell recording (Fig. 2b and Supplementary Fig. 6a). The pre-activated current was identical to native or amplified CRAC currents in its inwardly rectifying *I*-*V* shape, its selectivity for Ca²⁺ and its sensitivity to block by 5 nM Gd³⁺ (Fig. 2a, b and Supplementary Fig. 6b, c). However, the pre-activated current induced by C-Stim plus GFP-Orai declined to a half-maximal value in 34 ± 9 s (*n* = 14 cells), probably owing to pipette dialysis resulting in dilution and unbinding of cytosolic C-Stim, which, unlike full length Stim, is not constrained to the ER membrane while interacting with Orai. Indeed, when small pipettes with higher series resistance

and correspondingly slower diffusional access were used, the decline of the pre-activated current proceeded more slowly (Supplementary Fig. 6d, e).

We next examined the localization of GFP-Orai in relation to co-expressed C-Stim or Stim (Fig. 2c and Supplementary Fig. 7). Immunostaining of cytosolic C-Stim showed it was present in a ring near the surface membrane and was co-localized with GFP-Orai, suggestive of a constitutive coupling. Notably, no punctae of C-Stim and co-expressed GFP-Orai were observed, even though CRAC channels were constitutively active. In contrast to this homogeneous distribution of C-Stim and co-expressed Orai, co-localized full-length Stim and Orai showed distinct punctae as expected after Ca²⁺ store depletion. The C-terminal portion of Stim includes the coiled-coil motif involved in dimerization but lacks the amino-terminal sterile alpha motif domain responsible for higher order Stim aggregation after store depletion. We have previously shown by co-immunoprecipitation that store depletion induces a dynamic coupling between Stim and Orai¹². Here, we further demonstrate that *Drosophila* C-Stim physically interacts with Orai independently of the ER Ca²⁺ store content (Supplementary Fig. 8). Moreover, western blots after maleimide 1,6-bismaleimidohexane (BMH) cross-linking of intact cells demonstrated that C-Stim induces a shift towards higher order Orai homomultimers, including a clear tetramer population that was not observed when Orai was expressed alone (Fig. 2d). Collectively, these experiments show that C-Stim expressed as a cytoplasmic protein associates with and constitutively activates Orai subunits in the plasma membrane without forming punctae, and they provide evidence that the oligomeric state of Orai is dependent on C-Stim binding.

To determine Orai stoichiometry at the single-molecule level in the native membrane environment of intact cells, we used a recently

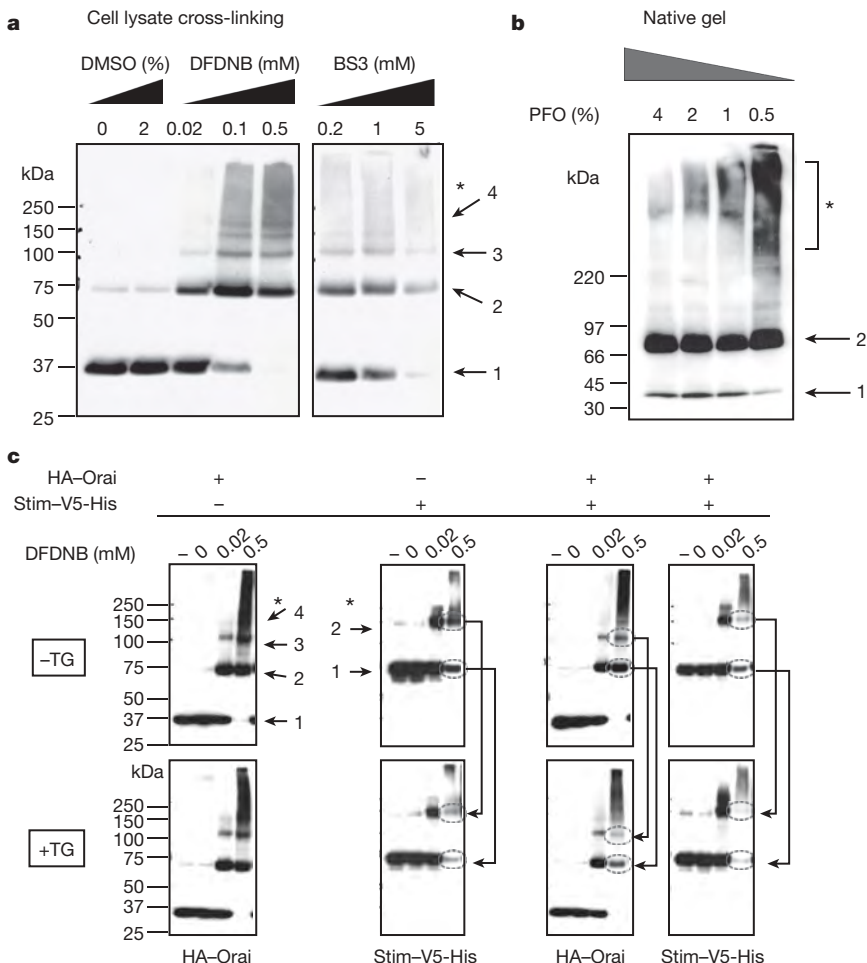


Figure 1 | Orai is mainly present as homodimers in resting S2 cells. Each panel is representative of at least 3 independent experiments. Numbers represent the assigned state of oligomerization: 1, monomer; 2, dimer; 3, trimer; 4, tetramer. Asterisks denote high-order aggregates.

a, Determination of Orai oligomeric structure using chemical cross-linking. DFDNB (1,5-difluoro-2,4-dinitrobenzene, membrane permeant) and BS3 (bis(sulfosuccinimidyl)suberate, membrane impermeant) were incubated with HA-Orai-transfected S2 cell lysates and the sizes of the cross-linked products were analysed by SDS-PAGE on 4–12% gradient gels. Orai oligomers, from dimer to tetramer, were observed with the dimer always being the predominant population. Similar results were obtained in intact cells using DSP (dithiobis(succinimidyl propionate), membrane permeant, data not shown), DFDNB (see Supplementary Figs 2 and 3) and the cysteine-reactive cross-linker BMH (membrane permeable). **b**, Confirmation of Orai dimerization using PFO-PAGE. HA-Orai-transfected S2 cell lysates were incubated with sample buffer containing different PFO concentrations for 30 min at room temperature before electrophoresis. **c**, DFDNB cross-linking of total cell lysates of S2 cells transfected with HA-Orai, with Stim-V5-His or co-transfected. Labels indicate untreated cells (-), dimethylsulphoxide (DMSO) vehicle control (0) and concentrations of DFDNB. Arrows show the reduction in Stim and Orai low-order oligomers upon Ca²⁺ store depletion by thapsigargin (1.5 μM for 15 min).

developed method²³ of total internal reflection microscopy (TIRFM) to image bleaching steps of individual GFP-tagged Orai. *Xenopus* oocytes were injected with complementary RNA (cRNA) for GFP-Orai with or without coincident injection of cRNA for Stim or C-Stim. When Stim was co-expressed, depletion of the Ca^{2+} store with thapsigargin resulted in clustering of GFP-Orai in punctae (Fig. 3a), making single molecules difficult to resolve. However, consistent with the results described earlier in *Drosophila* S2 cells, oocytes expressing both GFP-Orai and C-Stim showed a large Ca^{2+} influx as assessed by Ca^{2+} fluorimetry, together with the activation of an

endogenous Ca^{2+} -dependent Cl^- current, whereas neither Orai nor C-Stim alone were effective (Fig. 3b). Moreover, TIRFM imaging of GFP-Orai-expressing oocytes showed numerous diffraction-limited fluorescent spots (Fig. 3c) that were absent in the non-injected oocytes and increased in density with the time of expression. Continuous exposure to laser excitation resulted in stepwise decrements of fluorescence at these spots (Supplementary Videos 1 and 2) corresponding to bleaching of individual GFP molecules²³. Different spots showed varying numbers of bleaching steps, ranging from one to a maximum of four (Fig. 4a, b). Notably, estimates of the mean

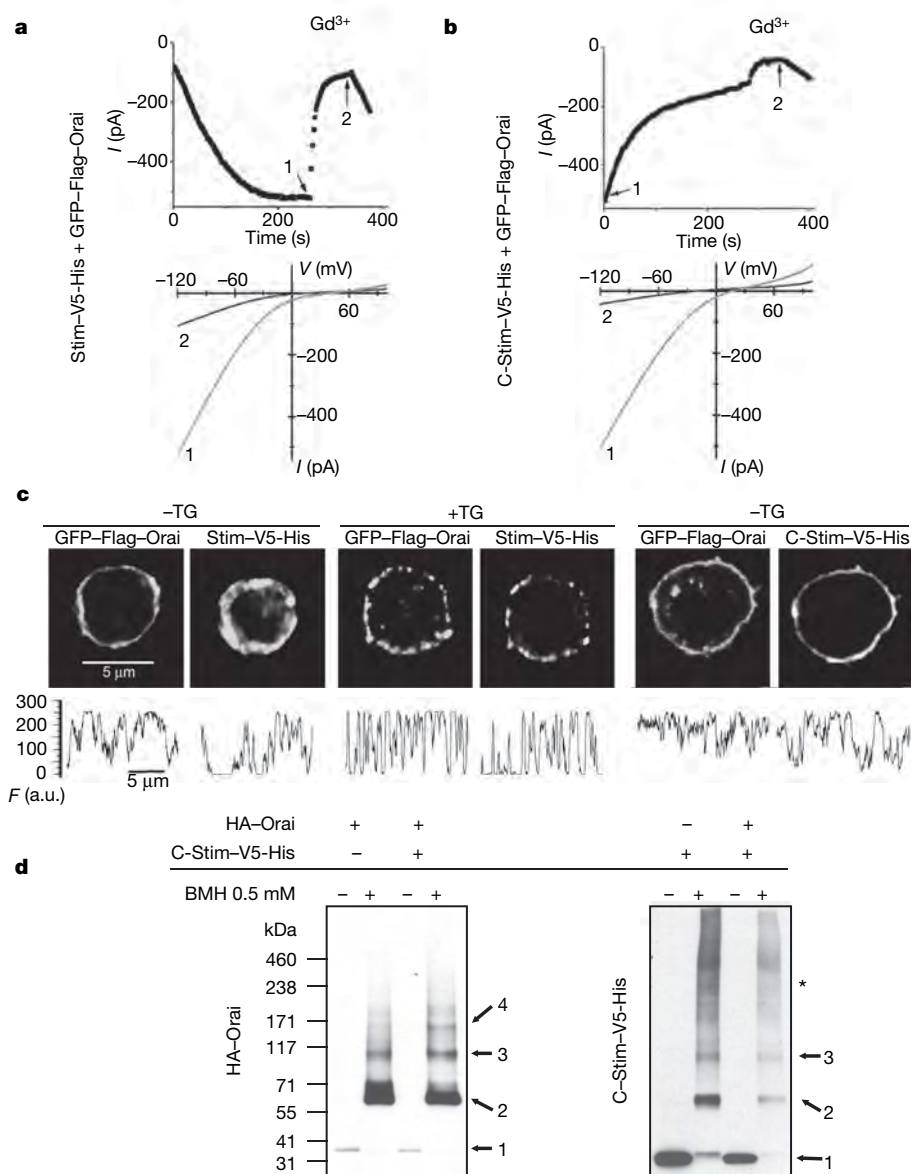


Figure 2 | The C terminus of Stim (C-Stim) constitutively activates Orai without forming punctae. **a, b**, Time course (top graphs) and I - V curves (bottom graphs) comparing the CRAC current in representative cells co-transfected with Stim + GFP-Orai (**a**) or with C-Stim + GFP-Orai (**b**). Application of 5 nM Gd^{3+} reversibly blocked most of the current in cells transfected either with Stim + GFP-Orai or with C-Stim + GFP-Orai. **c**, Subcellular localization of GFP-Orai together with Stim-V5-His or C-Stim-V5-His in resting (Stim-V5-His and C-Stim-V5-His) or store-depleted (2 μM thapsigargin for 15 min, Stim-V5-His only) co-transfected S2 cells. Puncta formation was only observed after store-depletion in cells expressing Stim-V5-His and GFP-Orai. The graphs underneath each picture show the fluorescence intensity profiles (F) for Orai and Stim obtained from the same regions of interest, tracing the perimeter of each cell clockwise from the top. a.u., arbitrary units. To quantify the extent to which

GFP-Orai was inhomogeneously distributed, we calculated the ratio of fluorescence variance to mean fluorescence from profiles such as those illustrated. Mean ratio values for GFP-Orai (\pm s.e.m.; $n = 6$ cells for each condition) were: Stim-V5-His - thapsigargin (TG), 29.03 ± 2.9 ; Stim-V5-His + thapsigargin, 62.9 ± 4.5 ($P = 0.00002$); C-Stim-V5-His - thapsigargin, 22.4 ± 3.7 (not significantly different from Stim-V5-His). **d**, BMH cross-linking in intact S2 cells transfected with HA-Orai, with C-Stim-V5-His or co-transfected with both. Numbers represent the inferred state of oligomerization: 1, monomer; 2, dimer; 3, trimer; 4, tetramer. The asterisk denotes higher order aggregates. The cross-linking pattern of Orai showed a clear tetrameric population when co-expressed with C-Stim but not in the absence of C-Stim. The cross-linking profile of C-Stim was not affected by the presence of Orai, and appeared mostly as dimers and trimers.

number of GFP molecules per spot made in this way differed markedly depending on the expression of C-Stim. In the oocytes expressing GFP–Orai alone, most of the spots (~70%) showed two steps to complete bleaching (Fig. 4a, c)—consistent with biochemical

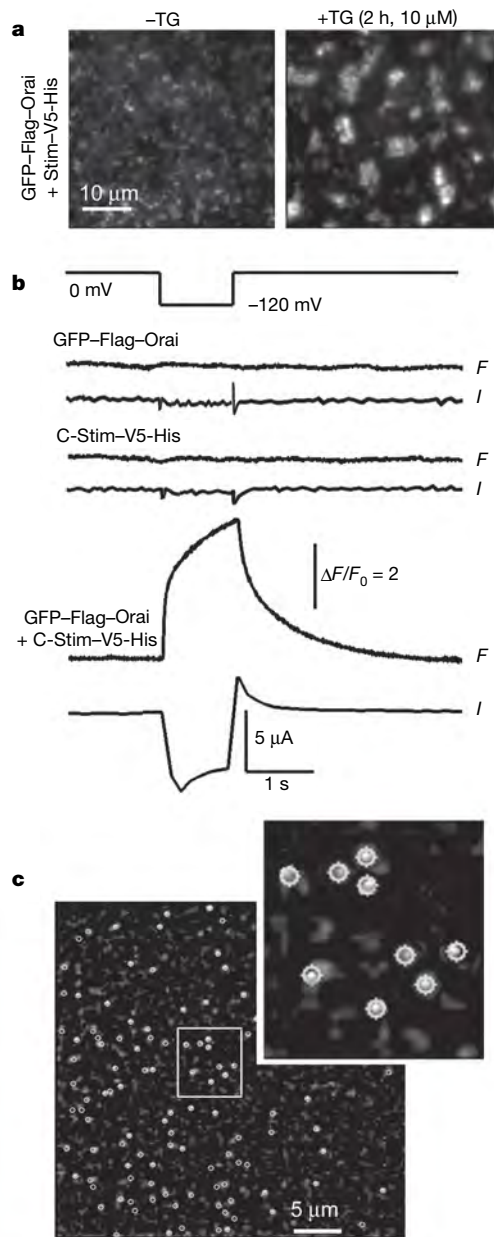


Figure 3 | Single-molecule photobleaching of GFP–Orai in intact oocytes. **a**, Store depletion induces the formation of Orai punctae in *Xenopus* oocytes. Images were obtained by TIRFM of oocytes expressing GFP–Orai together with Stim–V5–His and show $40 \times 40 \mu\text{m}$ regions in the animal hemisphere before (left) and 2 h after (right) bath application of 10 μM thapsigargin (TG) in zero-calcium Ringer’s solution. **b**, Oocytes expressing GFP–Orai together with C–Stim showed strong Ca^{2+} influx, whereas this was absent with expression of GFP–Orai or C–Stim alone. The pairs of traces show cytosolic $[\text{Ca}^{2+}]$ as reported by normalized fluorescence pseudo-ratio changes of Fluo-4 (*F*) and whole-cell voltage-clamp measurements of Ca^{2+} -activated Cl^- current (*I*) in response to a hyperpolarizing step from 0 mV to -120 mV (top trace). **c**, Representative TIRFM image, acquired before photobleaching, showing fluorescent spots (circled) sparsely distributed in the membrane of an oocyte expressing GFP–Orai together with C–Stim. The inset shows a magnified view of a small region (white box), with circular regions of interest used to measure bleaching steps overlaid on the image.

4

observations in S2 cells—whereas after co-expression with C–Stim, most spots (~62%) showed four-step bleaching (Fig. 4b, c). The small proportions of spots that showed one- or three-step bleaching may reflect instances of near-simultaneous stochastic bleaching steps that could not be separately resolved, or expression of non-fluorescent GFP molecules²³. The optical resolution of the microscope (approximately 250 nm) is inadequate to determine whether a spot showing four bleaching steps is truly a tetramer or, for example, two

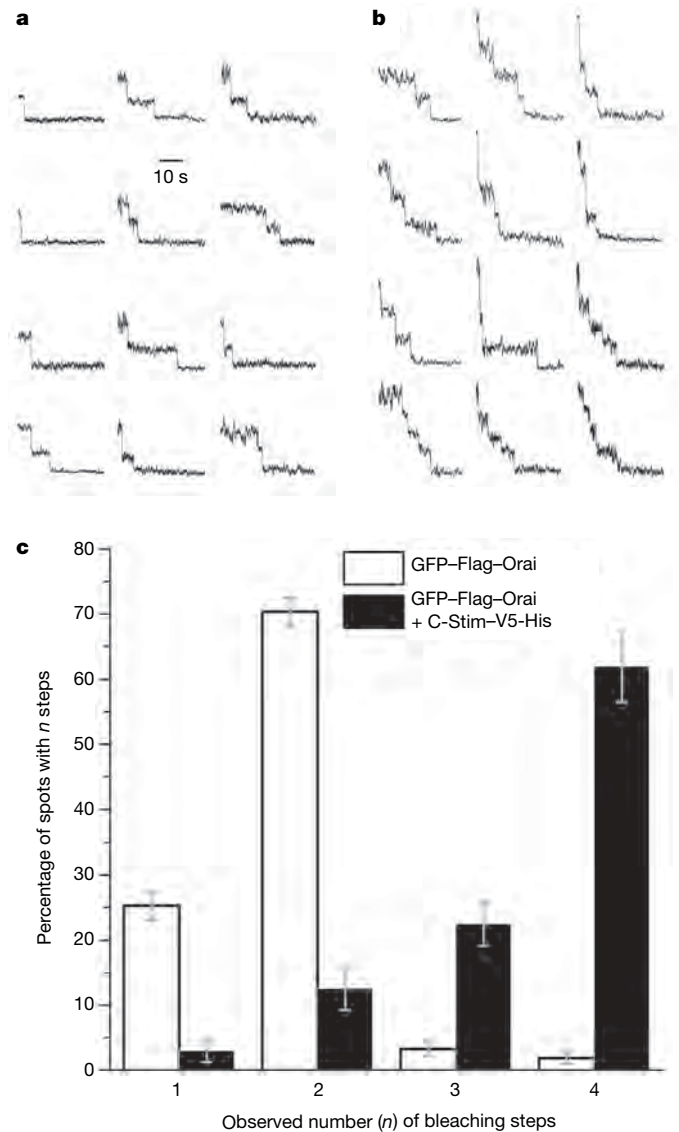


Figure 4 | GFP–Orai forms dimers in the basal state and mainly tetramers when co-expressed with C–Stim. **a**, **b**, Representative examples of single-molecule bleaching records obtained from oocytes expressing GFP–Orai alone (**a**) or GFP–Orai together with C–Stim (**b**). **c**, Histogram shows the percentages of spots that showed one, two, three and four bleaching steps in oocytes expressing GFP–Orai alone (open bars) and GFP–Orai plus C–Stim (filled bars). Errors bars indicate ± 1 s.e.m. Data for GFP–Orai were obtained from 400 spots, 11 imaging records and 6 oocytes; data for GFP–Orai + C–Stim were obtained from 278 spots, 5 imaging records and 3 oocytes. Comparison of bleaching step distributions with and without C–Stim yielded a Chi-square value of 590, $P < 0.001$. This cannot be attributed to an increased likelihood of two GFP–Orai dimers happening to occur indistinguishably close to each other owing to an increased expression level or to C–Stim-induced clustering, because fluorescence spots in both conditions showed similar random distributions and densities (respectively, 37 ± 6 and 41 ± 4 spots in a $40 \times 40 \mu\text{m}^2$ region), and we did not observe spots with more than four bleaching steps as might be expected for a macromolecular clustering.

distinct dimers linked by C-Stim. We favour the former interpretation on the basis of the evidence¹⁵ that the expression of an Orai1 tandem-tetramer construct forms functional CRAC channels, and that CRAC is inhibited when one subunit in the tetramer is replaced by a dominant-negative Orai. Thus, Orai is present in the membrane predominantly as dimers under basal conditions, and activation by C-Stim induces association to form tetramers.

Taken together, our results show that Orai adopts different quaternary structures depending on its activation state. In resting cells, Orai is present in the plasma membrane as a dimer, forming stable structural units, but when CRAC is activated, Orai is found predominantly as a tetramer. This result reconciles biochemical evidence pointing to a stable Orai dimer¹⁴ (Fig. 1) with electrophysiological evidence from tandem constructs indicating a tetrameric channel¹⁵. Moreover, we show that the coiled-coil C-terminal domain of Stim is sufficient to trigger dimerization of Orai dimers to form the functional tetrameric channel and to activate CRAC influx. However, at present we cannot distinguish whether this dimer to tetramer transition is sufficient to activate Orai channel activity, or if a Stim-induced conformational change in each subunit of Orai is further required for channel activity. The channel assembly and activation mechanism identified here is mechanistically unique in its requirement for an activator protein (Stim) to assemble and open the Orai tetrameric channel in the plasma membrane.

Note added in proof: A recent study²⁴ reported a tetrameric Orai1 stoichiometry of the CRAC channel by Fluorescence imaging methods.

METHODS SUMMARY

Drosophila S2 cells (Invitrogen) and HEK293 cells (American Type Culture Collection, ATCC) were propagated and transfected (see complementary DNAs described in Methods) as described previously^{2,12}. Chemical cross-linking was performed as described¹⁷ with minor modifications (see Methods). Cross-linking experiments were also performed on living S2 cells directly incubated with different concentrations of cross-linkers. Protein complexes were fractionated by PFO-PAGE as described previously^{17,19} and in Methods. Co-immunoprecipitations were performed in S2 cells as described¹² or on cells solubilized in PBS, 1% NP-40 and 5 mM EDTA for Stim–Orai interaction analysis. Equal amounts of protein were immunoprecipitated with the antibodies specified in the figure legends. After extensive washing, eluted samples were analysed by western blotting. Constructs and tags are described in Methods.

Transfected S2 cells were selected for whole-cell recording by fluorescence of GFP–Flag–Orai. Handling of C-Stim-transfected cells, solution recipes, voltage stimuli and data acquisition protocols are included in Methods.

Single-molecule bleaching experiments were performed on defolliculated *Xenopus* oocytes that had been injected 12–24 h previously with cRNAs for GFP–Orai alone or together with C-Stim–V5–His. Calcium influx was assayed by applying voltage-clamped hyperpolarizing pulses at the same time as monitoring the Ca²⁺-activated Cl[−] current and fluorescence of intracellularly loaded Fluo-4. Individual GFP–Orai multimers were visualized by TIRFM and image sequences were analysed by placing small regions of interest around fluorescence spots to manually count the bleaching steps during continuous exposure to 488 nm laser light.

Full Methods and any associated references are available in the online version of the paper at www.nature.com/nature.

Received 7 May; accepted 15 August 2008.

Published online 28 September 2008.

- Liou, J. *et al.* STIM is a Ca²⁺ sensor essential for Ca²⁺-store-depletion-triggered Ca²⁺ influx. *Curr. Biol.* **15**, 1235–1241 (2005).
- Roos, J. *et al.* STIM1, an essential and conserved component of store-operated Ca²⁺ channel function. *J. Cell Biol.* **169**, 435–445 (2005).
- Feske, S. *et al.* A mutation in Orai1 causes immune deficiency by abrogating CRAC channel function. *Nature* **441**, 179–185 (2006).

- Zhang, S. L. *et al.* Genome-wide RNAi screen of Ca²⁺ influx identifies genes that regulate Ca²⁺ release-activated Ca²⁺ channel activity. *Proc. Natl Acad. Sci. USA* **103**, 9357–9362 (2006).
- Vig, M. *et al.* CRACM1 is a plasma membrane protein essential for store-operated Ca²⁺ entry. *Science* **312**, 1220–1223 (2006).
- Cahalan, M. D. *et al.* Molecular basis of the CRAC channel. *Cell Calcium* **42**, 133–144 (2007).
- Lewis, R. S. The molecular choreography of a store-operated calcium channel. *Nature* **446**, 284–287 (2007).
- Zhang, S. L. *et al.* STIM1 is a Ca²⁺ sensor that activates CRAC channels and migrates from the Ca²⁺ store to the plasma membrane. *Nature* **437**, 902–905 (2005).
- Wu, M. M., Buchanan, J., Luik, R. M. & Lewis, R. S. Ca²⁺ store depletion causes STIM1 to accumulate in ER regions closely associated with the plasma membrane. *J. Cell Biol.* **174**, 803–813 (2006).
- Prakriya, M. *et al.* Orai1 is an essential pore subunit of the CRAC channel. *Nature* **443**, 230–233 (2006).
- Vig, M. *et al.* CRACM1 multimers form the ion-selective pore of the CRAC channel. *Curr. Biol.* **16**, 2073–2079 (2006).
- Yeromin, A. V. *et al.* Molecular identification of the CRAC channel by altered ion selectivity in a mutant of Orai. *Nature* **443**, 226–229 (2006).
- Muik, M. *et al.* Dynamic coupling of the putative coiled-coil domain of Orai1 with STIM1 mediates Orai1 channel activation. *J. Biol. Chem.* **283**, 8014–8022 (2008).
- Gwack, Y. *et al.* Biochemical and functional characterization of Orai proteins. *J. Biol. Chem.* **282**, 16232–16243 (2007).
- Mignen, O., Thompson, J. L. & Shuttleworth, T. J. Orai1 subunit stoichiometry of the mammalian CRAC channel pore. *J. Physiol. (Lond.)* **586**, 419–425 (2008).
- Hoenderop, J. G. *et al.* Homo- and heterotetrameric architecture of the epithelial Ca²⁺ channels TRPV5 and TRPV6. *EMBO J.* **22**, 776–785 (2003).
- Kedei, N. *et al.* Analysis of the native quaternary structure of vanilloid receptor 1. *J. Biol. Chem.* **276**, 28613–28619 (2001).
- Raab-Graham, K. F. & Vandenberg, C. A. Tetrameric subunit structure of the native brain inwardly rectifying potassium channel K_{ir} 2.2. *J. Biol. Chem.* **273**, 19699–19707 (1998).
- Ramjeesingh, M., Huan, L. J., Garami, E. & Bear, C. E. Novel method for evaluation of the oligomeric structure of membrane proteins. *Biochem. J.* **342**, 119–123 (1999).
- Huang, G. N. *et al.* STIM1 carboxyl-terminus activates native SOC, I_{crac} and TRPC1 channels. *Nature Cell Biol.* **8**, 1003–1010 (2006).
- Zhang, S. L. *et al.* Store-dependent and -independent modes regulating CRAC channel activity of human Orai1 and Orai3. *J. Biol. Chem.* **283**, 17662–17671 (2008).
- Yeromin, A. V., Roos, J., Stauderman, K. A. & Cahalan, M. D. A store-operated calcium channel in *Drosophila* S2 cells. *J. Gen. Physiol.* **123**, 167–182 (2004).
- Ulbrich, M. H. & Isacoff, E. Y. Subunit counting in membrane-bound proteins. *Nature Methods* **4**, 319–321 (2007).
- Ji, W. *et al.* Functional stoichiometry of the unitary calcium-release-activated calcium channel. *Proc. Natl Acad. Sci. USA*. doi:10.1073/pnas.0806499105 (29 August 2008).

Supplementary Information is linked to the online version of the paper at www.nature.com/nature.

Acknowledgements We thank L. Forrest for assistance in cell culture; T. Holmes and S. Leverrier for discussion during the course of the study; A. Amcheslavsky, A. Froger, K. Kalman and K. Cahalan for help with oocytes; W. Jiang for assistance in some of the co-immunoprecipitation experiments; M. Ramjeesingh for help with the PFO-PAGE technique; F.-A. Rassendren for the P2X₂ construct; and E. Isacoff and M. Ulbrich for discussion and help during a pilot photobleaching study. This work was supported by grants from the National Institutes of Health (M.D.C. and I.P.) and by a fellowship from the George E. Hewitt Foundation (A.P.).

Author Contributions A.P. designed and performed cDNA and cRNA constructs, cell biology and all biochemical experiments. A.D. performed all experiments in oocytes and data analysis of single-molecule photobleaching. A.V.Y. was responsible for patch-clamp experiments and analysis. S.L.Z. made the C-Stim construct, performed Ca²⁺ imaging experiments and collaborated on co-immunoprecipitation experiments. O.S. provided general technical assistance. I.P. supervised single-molecule experiments on oocytes. M.D.C. provided advice and overall direction, and supervised project planning and execution. A.P., I.P. and M.D.C. wrote the paper.

Author Information Reprints and permissions information is available at www.nature.com/reprints. Correspondence and requests for materials should be addressed to M.D.C. (mcahalan@uci.edu).

METHODS

Cell culture and transfection. *Drosophila* S2 cells (Invitrogen) were propagated and transfected as described previously¹². Cells were used 16 h after transfection for immunocytochemistry and 36–96 h after transfection for patch-clamp, single-cell $[Ca^{2+}]_i$ imaging and biochemistry. HEK293 cells (ATCC) were maintained and propagated as recommended by the ATCC. HEK293 cells were transfected using Lipofectamine 2000 (Invitrogen) reagents and used after 48 h for biochemistry.

Molecular cloning and *in vitro* transcription. HA–Orai, Flag–Orai, Stim–V5–His and GFP constructs for *Drosophila* expression were described previously¹². The GFP–Flag–Orai fusion protein (GFP–Orai) was made by introducing by PCR a 5′ in-frame EcoRI site just after the starting methionine of the Flag–Orai coding sequence and ligating the fragment into the EcoRI–BamHI sites of a monomeric variant of the enhanced GFP (pEGFP-C2, Clontech) in which the A206K mutation²⁵ was introduced by site-directed mutagenesis (Quickchange site-directed mutagenesis kit, Stratagene). The resulting GFP–Flag–Orai coding sequence was subcloned between the EcoRI and the NheI sites of the pAc5.1/V5–His B *Drosophila* expression vector (Invitrogen). The C-terminal fragment of Stim (C-Stim, amino acids 315–570) was generated by introducing by PCR a NotI site followed by a methionine upstream of amino acid 315, and subcloning the resulting fragment between the NotI and the XhoI site of the pAc5.1/V5–His A vector (Invitrogen) as described previously for full-length Stim pAc5.1/D-STIM–V5–His (ref. 8). For HEK expression, *Drosophila* HA–Orai in pAc5.1/V5–His B was subcloned between the EcoRI and the XhoI sites of the pcDNA3.1/Zeo(+) mammalian expression vector (Invitrogen) and the rat ΔN -P2X₂ receptor in pcDNA3, which was a gift from F.-A. Rassendren²⁶.

Xenopus expression constructs were obtained by subcloning the NotI–BamHI GFP–Flag–Orai fragment between the corresponding sites of the pXLI vector²⁷ (gift from J. E. Hall), or by subcloning the NotI–PmeI Stim–V5–His or C-Stim–V5–His fragments between the NotI–EcoRI sites of PXLII. This vector contains the 5′- and 3′- untranslated regions of the *Xenopus laevis* β -globin gene with an internal multiple cloning site and a T3 promoter. Capped cRNAs were transcribed *in vitro* using T3 RNA polymerase (mMESSAGE mMACHINE kit, Ambion).

All mutants and constructs were verified by DNA sequencing on both strands and by analytical endonuclease restriction enzyme digestion; function was tested by whole cell patch-clamp recording and/or Ca^{2+} imaging.

Co-immunoprecipitation and western-blotting. Co-immunoprecipitation was performed in S2 cells as described¹² with some modifications. After treatment, 5–10 × 10⁶ cells were lysed in 300 μ l of either RIPA lysis buffer (Upstate) for Orai oligomerization experiments, or in PBS, 1% NP-40 and 5 mM EDTA for Stim–Orai co-immunoprecipitations, both supplemented with 1 × complete EDTA-free protease inhibitor mixture (Roche) and passed five times through a 26G needle. After 30 min of solubilization at 4 °C under agitation, lysates were centrifuged (16,000g, 10 min, 4 °C) and the supernatant was collected. Equal amounts of protein (250–500 μ g) were diluted at 0.5 μ g μ l⁻¹ in PBS and mixed with either anti-HA-probe monoclonal-antibody-conjugated agarose beads (5 μ l beads per 100 μ g total protein, Santa Cruz), anti-Flag M2 monoclonal-antibody-conjugated agarose beads (5 μ l beads per 100 μ g total protein, Sigma), anti-V5 monoclonal antibodies (1.25 μ g per 100 μ g total protein, Invitrogen), or anti-HA-probe monoclonal antibodies (1 μ g per 100 μ g total protein, Santa Cruz) overnight at 4 °C on a rotating wheel. For the non-conjugated antibodies, 25 μ l of UltraLink protein A/G beads (Pierce) were subsequently added and rocked for 2 h at 4 °C. Beads were washed five times (5 min at 4 °C) with 1 ml of RIPA lysis buffer containing 10% glycerol or PBS and 0.05% NP-40, and proteins were eluted by boiling in 2 × concentrated LDS sample buffer (Invitrogen) supplemented with 100 mM dithiothreitol (DTT). Samples were resolved by SDS–PAGE on a 4–12% NuPAGE gradient gel (Invitrogen) and analysed by standard western blotting techniques. Cells transfected individually with each plasmid were used as controls, and immunodepletion of all samples was checked by SDS–PAGE of the flow through protein.

Immunoblots were incubated with the primary antibodies indicated, including: mouse anti-HA peroxidase-coupled antibody (Roche; 1:500) in PBS plus 0.5% casein blocking solution (Bio-Rad), for 1 h at room temperature; mouse anti-HA probe antibody (SantaCruz; 1:500) in PBS plus 0.5% casein, overnight at 4 °C; mouse anti-FlagM2 peroxidase-coupled antibody (Sigma; 1:2,500) in PBS plus 0.05% Tween-20, for 1 h at room temperature; mouse anti- α -tubulin DM1A antibody (Sigma; 1:2,000) in PBS plus 0.1% casein, for 2 h at room temperature; and mouse anti-V5 peroxidase-coupled antibody (Invitrogen; 1:5,000) in PBS plus 0.5% casein, for 1 h at room temperature. Proteins were detected by developing with the ECL+ detection kit (GE Healthcare).

Chemical cross-linking. The following homobifunctional reagents (Pierce) were used for protein cross-linking studies: the lysine-reactive

N-hydroxysuccinimide esters BS3 (water-soluble, non-membrane-permeable, spacer arm length 11.4 Å) and DSP (water-insoluble, membrane permeable, spacer arm length 12 Å), the lysine-reactive aryl halide DFDNB (water-insoluble, membrane permeable, spacer arm length 3 Å) and the cysteine-reactive BMH (water-insoluble, membrane permeable, spacer arm length 11.4 Å). All reagents were dissolved in PBS or DMSO immediately before use.

Chemical cross-linking was performed as described¹⁷ with some modifications. The cell cultures were collected and rinsed twice with ice-cold PBS and then sonicated in ice-cold cross-linking buffer (PBS pH 8 for lysine-reactive cross-linkers or PBS pH 7.4 and 2.5 mM EDTA for cysteine-reactive reagent) containing protease inhibitors (complete-mini EDTA-free, Roche). The protein content was measured by a micromethod using the Bio-Rad protein assay. Fifteen micrograms of proteins in an equal volume of cross-linking buffer were incubated with different concentrations of cross-linkers indicated in the figure legend or with the same volume of vehicle. Incubation was performed for 10 min at 37 °C and stopped by the addition of 20 mM Tris, pH 7.5, for the lysine-reactive cross-linkers. Alternatively, for the cysteine-reactive BMH, the treatment was performed for 20 min at room temperature and ended by the addition of 25 mM DTT. The quenched samples were subsequently mixed with 4 × concentrated Nu-PAGE sample buffer containing 50 mM DTT (Invitrogen), incubated at 70 °C for 10 min, and then subjected to electrophoresis. The samples were separated on 4–12% gradient Nu-PAGE Bis-Tris gels or 3–8% gradient Nu-PAGE Tris-acetate gels and analysed by western blotting.

Cross-linking experiments were also performed on living S2 cells. Cells (5 × 10⁶) were resuspended in 1 ml of cross-linking buffer and directly incubated with different concentrations of cross-linkers as described previously. After quenching, cell lysates were prepared and analysed by western blotting.

PFO–PAGE. Proteins complexes were fractionated by PFO–PAGE as described^{17,19}. Total cell lysates were prepared as for chemical cross-linking experiments. In some experiments, cell were lysed in the presence of 1% of the mild NP-40 detergent for 20 min at 4 °C under agitation and centrifuged at 16,000g for 10 min to remove cellular debris. The lysates (30–40 μ g) at 2 μ g μ l⁻¹ were mixed with doubly concentrated PFO sample buffer (100 mM Tris-base, 2–8% NaPFO (Oakwood Products Inc.), 20% glycerol and 0.005% bromophenol blue, pH 8.0) plus 25 mM DTT. After 25 min of incubation at room temperature, the samples were vortex mixed, centrifuged for 5 min at 10,000g and then subjected to electrophoresis on 4–12% precast gradient Novex Tris-Glycine gels (Invitrogen) with a running buffer containing 25 mM Tris, pH 8.5, 192 mM glycine and 0.5% NaPFO, adjusted with sodium hydroxide and electroblotted as described¹⁹. As molecular mass standards, the high-molecular-mass rainbow marker kit (GE Healthcare), cross-linked albumin and phosphorylase *b* (Sigma) were resuspended in PFO sample buffer, separated on the same gels, electroblotted and stained with amido black (Sigma). These methods were validated by showing that under the same experimental conditions and cellular context, the rat P2X₂ channel assembled as a trimer-hexamer (Supplementary Fig. 3b), in accordance with its previously described stoichiometry²⁸.

Immunocytochemistry. After washing in calcium-free Ringer, transfected S2 cells on poly-L-lysine-coated glass coverslips were treated for 10 min at room temperature with 1.5 μ M thapsigargin in calcium-free Ringer or left untreated in normal Ringer, fixed for 15 min at room temperature in 4% paraformaldehyde and 4% sucrose in PBS. Cells were washed in PBS containing 1% normal goat serum plus 50 mM glycine, and were then permeabilized in PBS containing 1% normal goat serum plus 0.05% Triton X-100. Blocking of nonspecific binding sites was performed by incubating cells with PBS containing 10% normal goat serum for 20 min and the primary antibody was added for 2 h at room temperature (anti-V5 mouse monoclonal antibody, Invitrogen; 1:200). After an extensive wash, cells were incubated for 25 min at 37 °C with Alexa-Fluor-conjugated secondary antibody (Alexa594 goat anti-mouse antibody, Invitrogen; 1:2,000). Stained cells were viewed by confocal microscopy (Zeiss LSM510 META). Background staining was determined by incubating non-transfected cells with both primary and secondary antibodies (data not shown).

Single-cell $[Ca^{2+}]_i$ imaging. Ratiometric Fura-2 $[Ca^{2+}]_i$ imaging was performed in S2 cells as described²⁸. Cells transfected with C-Stim were recognized by co-transfected GFP, with appropriate filters used to avoid contamination of Fura-2 fluorescence by bleed-through of GFP fluorescence. Data were analysed using METAFLUOR software (Molecular Devices) and ORIGINPRO 7.5 software (OriginLab) and are expressed as means \pm s.e.m.

Whole-cell recording. Patch-clamp experiments were performed in S2 cells at room temperature in the standard whole-cell recording configuration, as described¹². To decrease the Ca^{2+} influx caused by a preactivated CRAC current that might damage cells before recording or immunostaining, S2 cells co-transfected with C-Stim plus GFP–Orai, and control cells transfected with Stim plus GFP–Orai, were maintained for 16–96 h in complete calcium-free Schneider's insect medium (Sigma) and plated on poly-L-lysine-coated coverslips. For

whole-cell recording, cells were maintained in nominally Ca^{2+} -free external solution. After seal formation and just before break-in to achieve whole-cell recording, the standard 2 mM Ca^{2+} solution was applied locally to the cell. Pipette resistances were normally $\sim 2\text{ M}\Omega$, but pipettes ranging from 8 to 12 $\text{M}\Omega$ were used to evaluate diffusional access as a mechanism for run-down of constitutive CRAC currents induced by C-Stim expression. The recipes of external and internal solutions are indicated in Supplementary Table 1. Only cells with high input resistance ($>2\text{ G}\Omega$) were selected for recording. Membrane potentials were corrected for a liquid junction potential of 10 mV between the pipette and the bath solution. The series resistance was not compensated. The membrane potential was held at 0 mV, and 220-ms voltage ramps from -120 to 100 mV alternating with 220-ms pulses to -120 mV were delivered every 2 s. To calculate current densities, peak current amplitudes were divided by the membrane capacitance for each cell.

Oocyte preparation and cRNA injection. Plasmids containing cDNA clones coding for the *Drosophila* GFP-Flag-Orai and C-Stim-V5-His subunits were linearized and transcribed *in vitro*, and cRNAs were mixed to a final concentration of 0.001–0.01 $\mu\text{g}\mu\text{l}^{-1}$ and injected (30 nl) into defolliculated stage VI oocytes obtained from *Xenopus laevis*²⁹. After injection, oocytes were maintained for 12–24 h in Barth's solution (1.8 mM Ca^{2+}), and were then prepared for TIRFM imaging by manual removal of the vitelline membrane after shrinking in hypertonic 'stripping' solution (composition in mM: potassium aspartate, 200; KCl, 20; MgCl_2 , 1; EGTA, 10; HEPES, 10; pH 7.2, cooled to 4 °C).

Oocyte electrophysiology and Ca^{2+} measurement. Ca^{2+} influx was assayed using a two-electrode voltage clamp to apply hyperpolarizing steps to oocytes bathed in Ringer's solution with [Ca^{2+}] raised to 6 mM, and simultaneously measuring Ca^{2+} -activated Cl^- current³⁰ and monitoring cytosolic free [Ca^{2+}] by means of the fluorescence of Fluo-4 dextran loaded to a final intracellular concentration of $\sim 40\ \mu\text{M}$ ³¹.

Single-molecule GFP photobleaching and analysis. TIRFM of single GFP-Orai molecules expressed in *Xenopus* oocytes was accomplished using a home-built system²⁹ based around an Olympus IX70 microscope equipped with a $\times 60$, NA 1.45 TIRF objective. Devitellinated oocytes were allowed to settle on a cover glass forming the base of the recording chamber and were bathed in calcium-free

Ringer's solution (composition in mM: NaCl, 120; KCl, 2; MgCl_2 , 5; EGTA, 1; HEPES, 5; at pH 7.4). GFP-tagged molecules lying within the ~ 100 nm evanescent field were excited by total internal reflection of a 488 nm laser beam incident through the microscope objective. Images (128×128 pixel; 1 pixel = 0.33 μm) were acquired at 10 frames s^{-1} by a Cascade 128+ electron multiplying CCD camera (Roper Scientific). The resulting image stacks (1,000 frames; 100 s) were processed in MetaMorph (Molecular Devices) by averaging every two consecutive frames, followed by subtraction of a heavily smoothed (7×7 pixel) copy of each frame so as to correct for bleaching of autofluorescence and other background signals. Traces such as those in Fig. 4a, b were then obtained around selected spots, excluding those that showed obvious movement or where spots were too close to be unambiguously separated. The number of bleaching steps in each trace was determined by visual inspection, with measurements restricted to those spots that showed complete bleaching and where fluorescence steps could be clearly resolved above the noise level.

25. Zacharias, D. A., Violin, J. D., Newton, A. C. & Tsien, R. Y. Partitioning of lipid-modified monomeric GFPs into membrane microdomains of live cells. *Science* **296**, 913–916 (2002).
26. Newbolt, A. *et al.* Membrane topology of an ATP-gated ion channel (P2X receptor). *J. Biol. Chem.* **273**, 15177–15182 (1998).
27. Nielsen, P. A. *et al.* Molecular cloning, functional expression, and tissue distribution of a novel human gap junction-forming protein, connexin-31.9. Interaction with zona occludens protein-1. *J. Biol. Chem.* **277**, 38272–38283 (2002).
28. Aschrafi, A., Sadtler, S., Niculescu, C., Rettinger, J. & Schmalzing, G. Trimeric architecture of homomeric P2X₂ and heteromeric P2X₁₊₂ receptor subtypes. *J. Mol. Biol.* **342**, 333–343 (2004).
29. Demuro, A. & Parker, I. Optical single-channel recording: imaging Ca^{2+} flux through individual ion channels with high temporal and spatial resolution. *J. Biomed. Opt.* **10**, 11002 (2005).
30. Parker, I., Gunderson, C. B. & Miledi, R. A transient inward current elicited by hyperpolarization during serotonin activation in *Xenopus* oocytes. *Proc. R. Soc. Lond. B* **223**, 279–292 (1985).
31. Dargan, S. L., Demuro, A. & Parker, I. Imaging Ca^{2+} signals in *Xenopus* oocytes. *Methods Mol. Biol.* **322**, 103–119 (2006).